A Novel Control Scheme for Utility-Scale Inverter-Based Resources to Emulate Synchronous Generator Fault Response and Retain Existing Protection Infrastructure

Daniel Kelly*, Pratap Mysore†, Ned Mohan*
*University of Minnesota; †Pratap Consulting Services, LLC.

***Abstract*—This paper explores a novel control scheme for utility-scale inverter-based resources (IBR), which emulates synchronous generator behavior during fault conditions. This will ensure reliability of transmission-line protective devices, such as distance relays, which rely on the unbalanced currents traditionally produced by synchronous generators to accurately determine the fault location. As the generation profile of the grid continues to trend towards a higher penetration of renewables these relays will not be adequate, thus necessitating costly equipment upgrades. By implementing the proposed control scheme, existing relays will continue to operate properly and the need for any such equipment upgrades is eliminated.**

Keywords—Inverter Based Resources; utility-scale IBR; transmission-line protection; renewables; inverter control; protective relaying;

I. Introduction

Existing utility-scale IBRs, such as photovoltaics and wind turbines, are often controlled to generate balanced three-phase currents even during unbalanced faults (single-line to ground, line-to-line, double-line to ground) as well as balanced faults (three-line and three-lines to ground). However, the proper operation of commonly used protective relays relies on unbalanced currents produced by synchronous generators of conventional power plants [1]. With increasing penetration of IBRs towards the goal of one-hundred percent renewable generation, existing protection schemes may not be adequate [2-3].

The objective of this research is to enhance the integration of utility-scale IBRs by eliminating any costs related to protective equipment upgrades. Under the proposed inverter control scheme first the fault type is identified, then the inverters are controlled to produce unbalanced currents which emulate synchronous generator fault behavior. Through such emulation, the phase relationship between voltage and current is modified such that protective relays will operate properly. Thus, the existing transmission-line protection infrastructure is unaffected by the evolving generation profile of the grid.

Other proposed methods attempt to solve this issue of distance relay mis-operation through negative-sequence current injection, such as in the German grid code VDE-AR-N-4120 [4]. This introduces additional complexity over the control method proposed in this paper, which simply emulates the synchronous generator fault response seen by existing protection schemes.

Section II describes how the inverter control scheme was developed and details the system under study. Section III explores the results of the control scheme's performance in a simulated system with a utility-scale aggregated model switching inverter, and the results of testing COMTRADE files (Common format for Transient Data Exchange) on modern relays. Section IV evaluates the overall effectiveness of the control scheme. Section V examines future extensions to this research.

II. Inverter Control Scheme to Emulate Synchronous Generator Fault Behavior

Successful emulation of synchronous generator behavior is achieved if the 345kV relay closest to the IBR meets the following conditions:

- The faulted phase voltage does not shift much with respect to its pre-fault angle.
- The faulted phase current lags the faulted phase voltage by approximately the line impedance angle.

A. *Synchronous Generator Fault Behavior*

To determine appropriate inverter reference currents during fault conditions, it was necessary to model a conventional power system to benchmark the desired behavior. A 100 MVA synchronous generator was connected to a 1000 MVA equivalent

NSF Sponsored Grant #1936560

source, representing the bulk power system, via a 345kV transmission line as shown in Fig. 1.

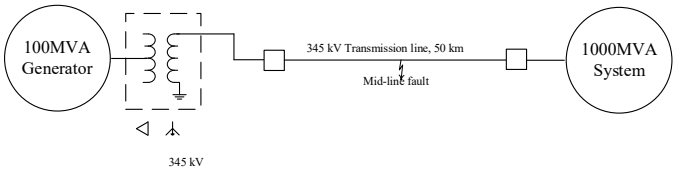

Fig. 1: System one-line with 100MVA generator

PSS@CAPE was selected as the modeling software, due to availability of realistic system data. Relevant system parameters are listed in Table 1.

Table 1: System parameters with synchronous generator

Gen. Voltage/Power	13.8 kV	100 MVA
Gen. Impedances	X_d" = 0.148 p.u.	X_2 = 0.141 p.u.
Xfmr Windings	13.8 kV Delta	345 kV Wye-Gnd
Xfmr Impedance	Z_1 = 0.126 p.u.	
Line Impedance	Z_1 = 2 + j19 Ω	Z_0 = 16 + j65 Ω
Line Length	50 km	
Eq. Source Power	345 kV	1000 MVA
Eq. Source Impedances	Z_1= 10.5+j117 Ω	Z_0= 15.6+j136 Ω

A mid-line fault was created for various fault types, and synchronous generator currents were recorded in Table 2. Prior to fault inception, the system was generating at unity power factor with the angle of phase-A on the 345kV transmission line at 0°.

Table 2: Synchronous generator fault currents

Fault Type	I_a (p.u.)	I_b (p.u.)	I_c (p.u.)
A-G	2.1 ∠ -85°	2.1 ∠ 95°	0.04 ∠ -113°
B-C	1.8 ∠ -177°	1.8 ∠ -175°	3.6 ∠ 4°
B-C-G	2.1 ∠ -146°	2.1 ∠ 153°	3.6 ∠ 4°
A-B-C-G	3.6 ∠ -117°	3.6 ∠ 123°	3.6 ∠ 3°

Note that the subscript case denotes the location of the measured signal. For example, I_a (lower case a) indicates the 690V phase-A current, and I_A (upper case A) indicates the 345kV phase-A current.

These currents were used as a basis for determining appropriate inverter reference currents in Section II-B. The resulting generator currents are a function of the system impedance which varies between transmission networks; therefore, the inverter currents need not identically replicate these results.

During the fault, the pre-fault voltage and the post-fault voltage phase angles do not change appreciably. For the inverter simulations, pre-fault voltage angle is used as a reference to shift the phase currents, with pre-determined phase angles based on the type of fault.

B. *Inverter Model and Reference Currents*

A 100 MW, 50 kHz SV-PWM inverter was modeled in Simulink and connected to the transmission network as shown in Fig. 2. For more details on the inverter model, please refer to [4].

Simulink was selected as the software due to its capability to model switching inverters and power systems. It is also compatible with Opal-RT, a platform that can run Simulink models in real-time and can easily generate COMTRADE files, which were used to export the simulation results for testing on distance relays.

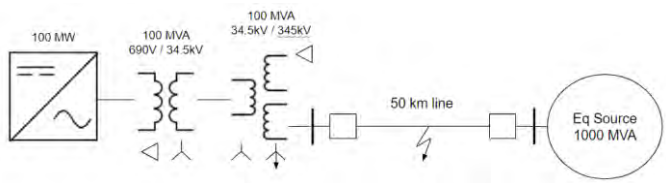

Fig. 2: System one-line with 100MW IBR

An additional 3-winding transformer was added to represent the configuration of a utility-scale IBR generation facility more accurately. The 2-winding transformer had an impedance of 5.75%, and the 3-winding transformer impedance was 10%. The transmission-line and equivalent source impedances are the same as in Table 1.

Inverter reference currents are limited to 1.0 per-unit, but still mimic the relative magnitudes and phase relationship of the synchronous generator currents. After a fault is detected, the inverter reference currents will be changed from their normal balanced, unity power factor operation to those shown in Table 3. This will result in the correct voltage/current phase relationship at the relay to accurately detect the fault location.

Table 3: Inverter currents with respect to V_A reference angle

Fault Type	I_a (p.u.)	I_b (p.u.)	I_c (p.u.)
A-G	1∠ -85°	1∠ 95°	0
B-C	0.5 ∠ 180°	0.5 ∠ 180°	1 ∠ 0°
B-C-G	0.5 ∠ -150°	0.5 ∠ 150°	1 ∠ 0°
A-B-C-G	1 ∠ -115°	1 ∠ 125°	1 ∠ 5°

For other faults in the same category, the reference currents are determined by maintaining the relative difference between each phase current angle, as well as between the pre-fault angle and post-fault angle for each current.

For example, a B-G fault would shift I_b by -85° (-120° - 85°) = -205°, with $I_c = -I_b$, and $I_a = 0$.

C. *Fault Identification*

Before inverter reference currents can be changed, the fault type must be correctly identified. This is accomplished by measuring 345kV phase (A-G, B-G, C-G) and line-to-line (A-B, B-C, C-A) voltage magnitudes at the relay location, classifying the fault according to the following criteria:

- Single-Line to Ground
  - Faulted phase below 0.8 p.u.
  - Healthy phases above 0.8 p.u.
- Line-to-Line
  - Both faulted phases below 0.8 p.u.
    - But above 0.4 p.u.
  - Faulted line-to-line below 0.8 p.u.
- Double-Line to Ground
  - Both faulted phases below 0.4 p.u.
  - Faulted line-to-line below 0.8 p.u.
- Three-Lines to Ground
  - All phases below 0.8 p.u.

The 0.8 per-unit threshold was selected because it is significantly below normal operating conditions, and the 0.4 per-unit threshold was selected to differentiate between a line-to-line and double-line-to-ground fault.

The RMS voltage magnitudes used for fault detection are calculated over a one cycle (60 Hz) moving window. This causes a misclassification when a double-line to ground fault occurs, as the voltage magnitudes of the faulted phases briefly meet the line-to-line criteria when they drop below 0.8 per-unit, but before they drop below 0.4 per-unit. A similar misclassification may briefly occur for a three-phase fault as a single-line to ground fault.

These misclassifications necessitate adding a delay of one cycle after a fault is first detected but before the inverter reference currents are changed, to allow for the voltage magnitudes to reach appropriate levels for accurate fault detection. This will be made clear in Section III-A.

III. Results

A. *Fault Detection*

Responsiveness of this control method is important to its success when implemented in a transmission network. As such, the time from fault inception to inverter current modification should be minimized, which in turn will minimize the fault clearing time.

The first parameter of concern is the time it takes to detect each type of fault. As mentioned in the previous section, this must also include a delay to avoid misidentification of fault types with similar criteria.

The magnitude of V_A at the relay drops below the 0.8 per-unit threshold 4.91ms after the fault creation, as shown in Fig. 3.

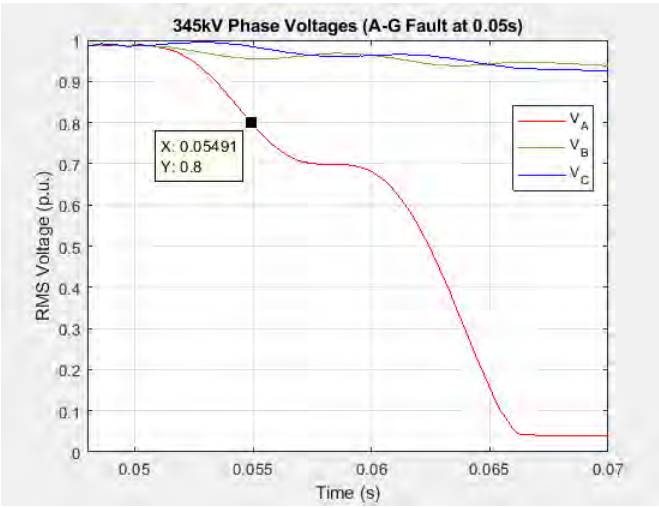

Fig. 3: 345kV phase voltage magnitudes during A-G fault

The time from fault detection to inception is well within one cycle. However, to avoid misclassification of fault types we must introduce an additional delay. Examining the RMS voltages for a three-phase to ground fault elucidates the vulnerability of this fault detection method without adding an additional delay.

Fig. 4 shows the RMS voltage magnitudes for a three-phase fault created at 0.05s. The magnitude of V_B drops below 0.8 per-unit before the other phases at 0.05329s, briefly causing a misclassification as a B-G fault. Not until the magnitude of V_C drops below 0.8 per-unit at 0.05691s is the fault correctly identified as a three-phase fault.

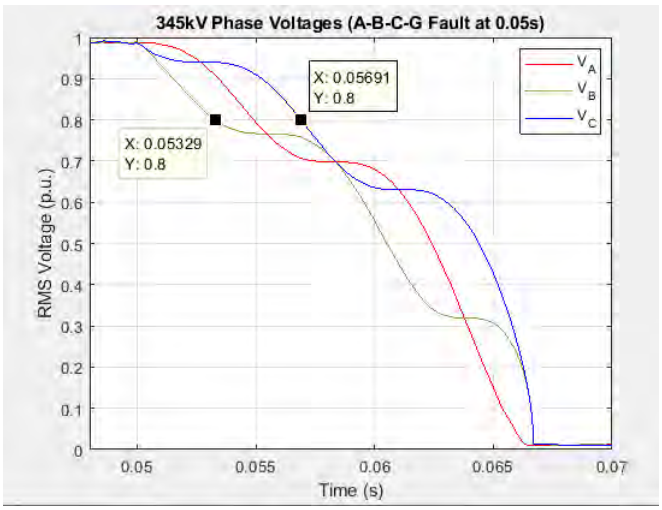

Fig. 4: 345kV phase voltage magnitudes during A-B-C-G fault

There is a 3.62ms delay between the misclassification and the correct classification. A one cycle delay (16.67ms) was selected to ensure a large safety margin to prevent any issues with misidentification of faults.

Table 4 summarizes the fault detection results, with the rightmost column showing the total time from fault inception to inverter reference current modification. The B-C fault has the longest total time of 24.58ms.

Table 4: Fault detection times, relative to fault inception

Fault Type	Initial Fault Detection (ms)	Added Delay (ms)	Reference Current Modification (ms)
A-G	4.91	16.67	21.58
B-C	7.91	16.67	24.58
B-C-G	3.29	16.67	19.96
A-B-C-G	3.29	16.67	19.96

B. Inverter Current Modification

Once the fault type has been correctly identified and the inverter reference currents modified, there will be some transient period. Fig. 5 shows the 690V inverter currents for during an A-G fault. For this study, it was assumed that the pre-fault IBR generation was 1.0 per-unit.

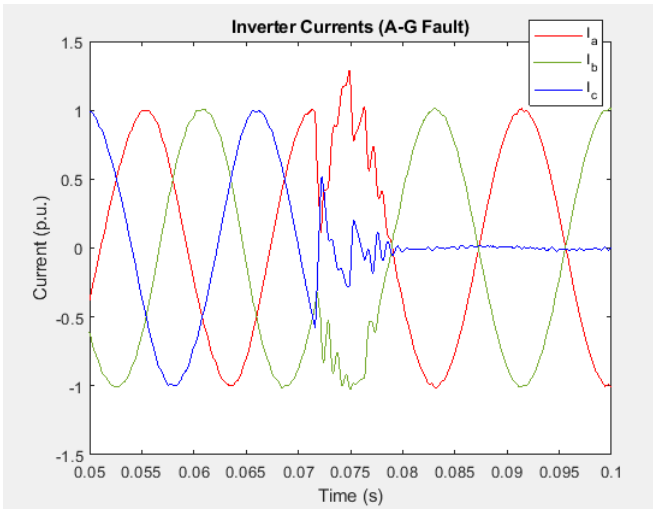

Fig. 5: Inverter currents during A-G fault

The fault is created at 0.05s, the leftmost point in Fig. 5. As expected, there is no change in inverter current until the inverter reference currents are changed 21.58ms after fault inception, per Table 4. This causes a transient response as inverter currents stabilize to their new reference values. The transient behavior resolves within 9ms of reference current modification, and within 2 cycles from fault inception. Specifically, transient resolution occurs at 28.9ms after the fault when $I_a = -I_b$ and $I_c \approx 0$.

The results for the remaining fault types are not remarkably different than A-G, so graphs of the current waveforms are omitted. Table 5 shows the relative time from fault inception until the transient period resolves into the desired inverter current behavior.

Table 5: Inverter current transient resolution time, relative to fault inception

Fault Type	Reference Current Modification (ms)	Transient Resolution (ms)
A-G	21.58	28.9
B-C	24.58	41.5
B-C-G	19.96	33.1
A-B-C-G	19.96	31.8

The B-C fault takes the longest of the four types from fault inception to inverter current transient resolution, completing in approximately 2.5 cycles.

C. *Verifying Synchronous Generator Emulation*

Recall that successful emulation of synchronous generator behavior in this paper was defined to be: 1) that the faulted phase voltage angle does not shift much with respect to its pre-fault angle, and 2) the faulted phase current lags the faulted phase voltage by the line impedance angle.

For an A-G fault, Fig. 6 shows the 345kV voltage waveforms. The angle of V_A shifts from 0° pre-fault to -8° post-fault, which is acceptably close enough to allow for proper relay operation.

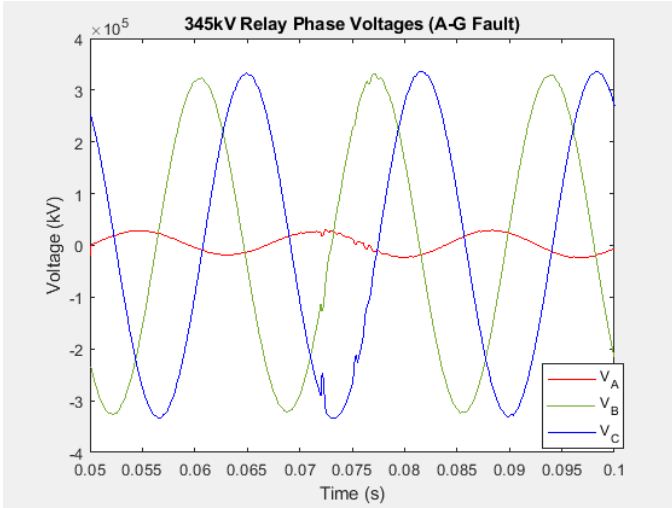

Fig. 6: 345kV relay phase voltages during A-G fault

For a synchronous generator to be emulated for an A-G fault, I_A should lag V_A by the line impedance angle. In the simulated transmission network, $\angle Z_{line} = 85°$. Fig. 7 shows that this relationship is indeed satisfied within 3 cycles and maintained thereafter.

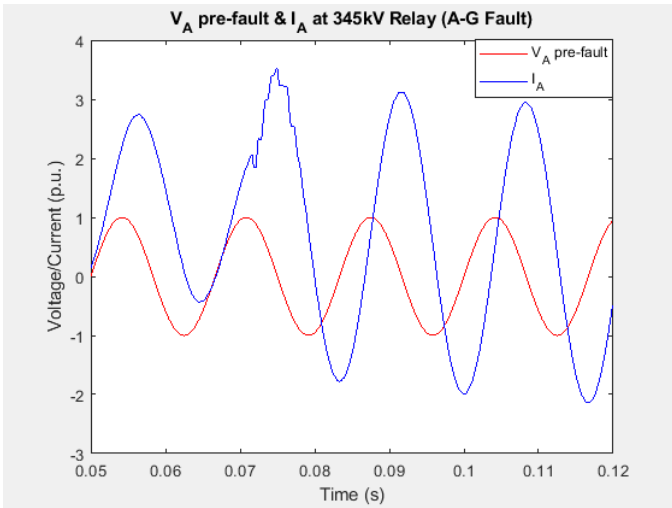

Fig. 7: 345kV voltage/current phase relationship at the relay (A-G fault)

As shown in the previous two figures, both conditions for satisfactory emulation of synchronous generator behavior have been met. Table 6 shows the 345kV phase relationships for all four types of faults, and specifically indicates which voltage and current signals are critical for each fault type.

Table 6: Faulted voltage and current phase relationships at 345kV relay

Fault Type	V	I
A-G	∠0° V_A	∠-85° I_A
B-C	∠-90° V_{BC}	∠-175° I_B
B-C-G	∠-90° V_{BC}	∠-250° I_B
A-B-C-G	∠0° V_A	∠-85° I_A

D. *Validating COMTRADE files*

The voltage and current data at the relay were exported to COMTRADE files. These files are played back on relays to test if they will operate when exposed to the recorded set of voltages and currents. The goal was to verify accurate fault location and operation of the Zone 1 distance element for a mid-line fault. Relays under testing were set to reach 80% of the line impedance for Zone 1 reach with no delay, and 120% of the line impedance for Zone 2 reach with a time delay operation.

To confirm that there was no overreach of the Zone 1 distance element, four additional simulations were run for an end-line fault of each type. Table 7 shows the measured fault distance and whether the Zone 1 element picked up for both mid-line and end-line faults. The distance measurement is represented in per-unit (0.5 p.u. = mid-line).

Table 7: COMTRADE validation results

Fault Type	Mid-Line		End-Line	
	Dist. (p.u.)	Zone-1?	Dist. (p.u.)	Zone-1?
A-G	0.493	Yes	0.991	No
B-C	0.503	Yes	0.995	No
B-C-G	0.562	Yes	1.048	No
A-B-C-G	0.502	Yes	1.009	No

IV. Conclusions

The profile of the electric grid will continue to move towards a higher penetration of IBRs, as local & state governments and utility companies set more ambitious renewable energy generation targets.

Existing distance relays in transmission networks are susceptible to failure as IBR penetration continues to increase, due to their reliance on unbalanced current generation of synchronous generators and phase relationship between voltages. By simply modifying inverter reference currents after a fault is detected, synchronous generator behavior expected by existing relays will be emulated, effectively eliminating any costs related to protective equipment upgrades.

The proposed novel inverter control method proved successful in the transmission network under study in this paper. All types of faults were accurately detected within one cycle, inverter currents modified within two to three cycles, and synchronous generator behavior replicated within three cycles, resulting in accurate fault distance measurements by the relay with no Zone 1 overreach. The proposed control scheme can be easily implemented in existing inverters and has the potential to be a de-facto standard in all future inverters.

V. Future Work

COMTRADE verification on additional relays. Due to COVID-19 protocols, it was difficult to obtain access to multiple manufacturer's relays for COMTRADE verification. It would be ideal to expand this verification to as many relays as possible.

Hardware verification in conjunction with Opal-RT's real time simulation capabilities. A low power inverter employing the proposed control scheme would be connected to the same transmission network simulated in this paper. Successful hardware verification would be an encouraging step towards testing this control scheme on commercially available inverters.

The impact of pre-fault IBR generation should be explored. This paper assumed that it was possible for the IBR to provide 1.0 per-unit current throughout the fault. If available solar or wind resources are low when the fault occurs, is there a

negative impact on this scheme? If so, what would be the required energy storage to mitigate these issues?

VI. References

[1] Paul M. Anderson, 1995, Analysis of Faulted Power Systems, IEEE Press.

[2] IEEE/NERC Task Force on Short-Circuit and System Performance Impact of Inverter Based Generation, Jul. 2018, Impact of inverter based generation on bulk power system dynamics and short-circuit performance, Tech. Rep. PES-TR68.

[3] NERC Inverter-Based Resource Performance Task Force (IRPTF), PRC-024-2 Gaps Whitepaper, NERC.

[4] VDE Forum Network Technology/Network Operation in the VDE, 2018, Technical Connection Rules for High-Voltage (VDE-AR-N 4120).

[5] Ned Mohan, 2014, Advanced Electric Drives: Analysis, Control, and Modeling Using MATLAB / Simulink, John Wiley & Sons.

VII. Biographies

Daniel Kelly: Daniel Kelly is a PhD student at the University of Minnesota with primary research interests in power systems, renewable energy, and power electronics. He has five years of industry experience as a power system engineer, focusing on power system protection, reliability, and safety. He received his BSECE and BSCS from the University of Kentucky, and MSECE from the University of Minnesota. He is a registered professional engineer in the state of Kentucky.

Pratap Mysore: Pratap Mysore has over 40 years of experience in power system protection and is a well-recognized figure in the area of protection and relaying in power systems. He has research experience working in Hindustan Brown Boveri (Now ABB) and has worked in two utilities including Xcel energy. He was the Director of Protection at HDR, a large consulting group and is now an independent consultant working with several utilities on power system protection. He has extensive experience in fault analysis in power networks. He is very active in developing industry standard documents while serving as a member, vice-chair and chair of working groups in the IEEE Power Systems Relaying and Control Committee (PSRC). He was the chair of PSRC during 2016-2018. He was also active in the working group from PSRC that developed a much needed technical report titled “Impact of Inverter-based generation on Bulk Power System Dynamics and Short Circuit performance” prepared by a joint task force consisting of the Power System Dynamics committee (PSDP), PSRC, and NERC.

Ned Mohan: Ned Mohan is Regents Professor at the University of Minnesota where he started teaching and doing research in 1976. He has written six textbooks on power electronics, power systems and electric machines/drives that have been translated into the cumulative of nine languages. He has guided 150 graduate students, including 47 PhDs. His research has earned him prestigious IEEE-PES Awards: Nari Hingorani FACTS Award, Ramakumar Family Award in Renewable Energy, and the PES Educator Award. He is a Life Fellow of the IEEE and a member of the National Academy of Engineering.